

VisLingInstruct: Elevating Zero-Shot Learning in Multi-Modal Language Models with Autonomous Instruction Optimization

Anonymous ACL submission

Abstract

This paper presents VisLingInstruct, a novel approach to advancing Multi-Modal Language Models (MMLMs) in zero-shot learning. Current MMLMs show impressive zero-shot abilities in multi-modal tasks, but their performance depends heavily on the quality of instructions. VisLingInstruct tackles this by autonomously evaluating and optimizing instructional texts through In-Context Learning, improving the synergy between visual perception and linguistic expression in MMLMs. Alongside this instructional advancement, we have also optimized the visual feature extraction modules in MMLMs, further augmenting their responsiveness to textual cues. Our comprehensive experiments on MMLMs, based on FlanT5 and Vicuna, show that VisLingInstruct significantly improves zero-shot performance in visual multi-modal tasks. Notably, it achieves a 15.9% increase in accuracy over the prior state-of-the-art on the ScienceQA dataset.

1 Introduction

The integration of Large Language Models (LLMs) with vision and multi-modality, epitomized by models like BLIP-2 (Chen et al., 2022; Alayrac et al., 2022; Li et al., 2023), has marked a significant evolution in the Natural Language Processing (NLP) field. This advancement led to the emergence of Multi-Modal Language Models (MMLMs), blending visual and linguistic data processing to enhance complex multimodal information understanding and generation. InstructBLIP (Dai et al., 2023), a notable example, utilizes advanced instruction tuning for image-text pairs, significantly improving the Q-Former module’s zero-shot learning capabilities in a variety of vision-language multi-modal tasks. This progression underscores the potential of MMLMs in navigating the intricacies of multi-modal data, setting a new benchmark in the intersection of language, vision, and machine learning.

However, the effectiveness of MMLMs is highly constrained by the quality of textual instructions. Current instruction-tuned models (Ouyang et al., 2022; Zheng et al., 2023b), effective as they may be, while potentially effective, introduces significant challenges, particularly for the users lacking expertise in crafting optimal instructions. The limitation leads to inconsistent and sometimes sub-optimal outputs, thus impeding the practical utility of MMLMs in the real world scenarios. To mitigate this issue, we propose a novel autonomous optimization method for textual instruction, named **Visual, Linguistic, Instruction** optimization (VisLingInstruct). VisLingInstruct introduces an innovative method through In-Context Learning (ICL) (Min et al., 2022) based on the comparison between instruction cases, using MMLMs’ linguistic capabilities to autonomously enhance and evaluate textual instruction. This method can guide the model towards generating more effective and contextually appropriate instructions.

Complementing our instructional optimization strategy, we present an architectural innovation aimed at enhancing the alignment between visual and textual modules within MMLMs. Inspired by recent advancements in models such as MiniGPT4 (Zhu et al., 2023), LLaVA (Liu et al., 2023b), mPLUG-Owl (Ye et al., 2023), and BLIVA (Hu et al., 2023), our architecture enhances the integration of textual and visual data. This integrative approach enables MMLMs to more effectively process and interpret complex tasks that require an understanding of both textual and visual elements, thereby improving accuracy and contextual understanding. Figure 1 offers a visual comparison of the alignment modules in different MMLMs, highlighting the distinctive features and benefits of our proposed method. Through this architectural enhancement, we aim to bridge the existing gaps in multi-modal data processing, creating a more cohesive and efficient model capable of tackling the

nuanced demands of multi-modal interactions.

In summary, our contributions are as follows:

- We introduce substantial architectural improvements for better integration of multi-modal data within MMLMs during training (Section 3.1).
- We present an autonomous method for optimizing instruction quality, tailored to improve the effectiveness of textual instruction during inference (Section 3.2).
- We conduct comprehensive experiments and ablation studies to demonstrate the effectiveness of VisLingInstruct and the success of each component. Notably, VisLingInstruct has improved the performance by a significant margin of 15.9% on the ScienceQA dataset.

2 Related Work

2.1 Instruction Tuning in MMLMs

Instruction tuning has emerged as a cost-effective alternative to the expensive pre-training of large models, focusing on fine-tuning a few foundational models for downstream tasks. In this context, models like InstructGPT (Ouyang et al., 2022), Flan-T5 (Chung et al., 2022), and Vicuna (Zheng et al., 2023b) represent significant strides in conversational models obtained through instruction tuning based on LLMs. These models have showcased exceptional question-answering capabilities, underscoring the importance of instruction-based approaches in language generation. In the multi-modal domain, advancements such as Mini-GPT4 (Zhu et al., 2023), LLaVA (Liu et al., 2023b), mPLUG-Owl (Ye et al., 2023), InstructBLIP (Dai et al., 2023), and BLIVA (Hu et al., 2023) have focused on instruction fine-tuning. These methods typically involve aligning images and text by introducing transitional layers, like Q-Former and fully connected layers, between visual encoders and LLMs. Our work builds upon these foundations, aiming to further optimize the instruction tuning process for enhanced performance in MMLMs.

2.2 Optimizing Instructions for Large Models

Historically, models akin to BERT (Kenton and Toutanova, 2019) have utilized prompt crafting techniques (Brown et al., 2020) to boost performance, with subsequent research exploring methods to discover higher-quality prompts (Gao et al.,

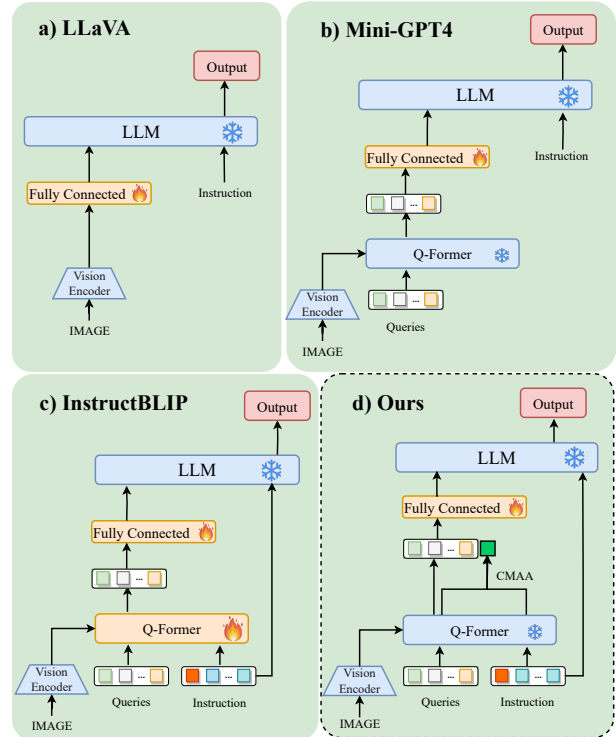


Figure 1: The structural comparison among the alignment modules of different MMLMs. The orange modules in the figure represent open weights, while the blue modules indicate frozen weights.

2021; Lu et al., 2023). In generative models, this concept has evolved into optimizing 'instructions', leading to a series of works focused on prompt and instruction optimization (Wei et al., 2022; Min et al., 2022). Notably, UPRISE (Cheng et al., 2023) trained a prompt retriever for acquiring superior instructions, while OPRO (Yang et al., 2023) conceptualized LLMs as optimizers, formulating optimization tasks in natural language. Zheng et al. introduced STEP-BACK prompting, enabling LLMs to derive higher-level concepts from detailed instances. To the best of our knowledge, we spearhead the manual-free optimization of textual instruction in zero-shot manner for a wide range of multi-modal tasks.

3 Methods

Our approach comprises two components: First, we refine the architecture of existing multi-modal models and their fine-tuning mechanisms to augment their perceptivity of instruction, that is, the Enhanced Multi-modal Alignment (EMA). Second, subsequent to the model's fine-tuning, we concentrate on the autonomous optimization of instructions during the inference, referred to as the Au-

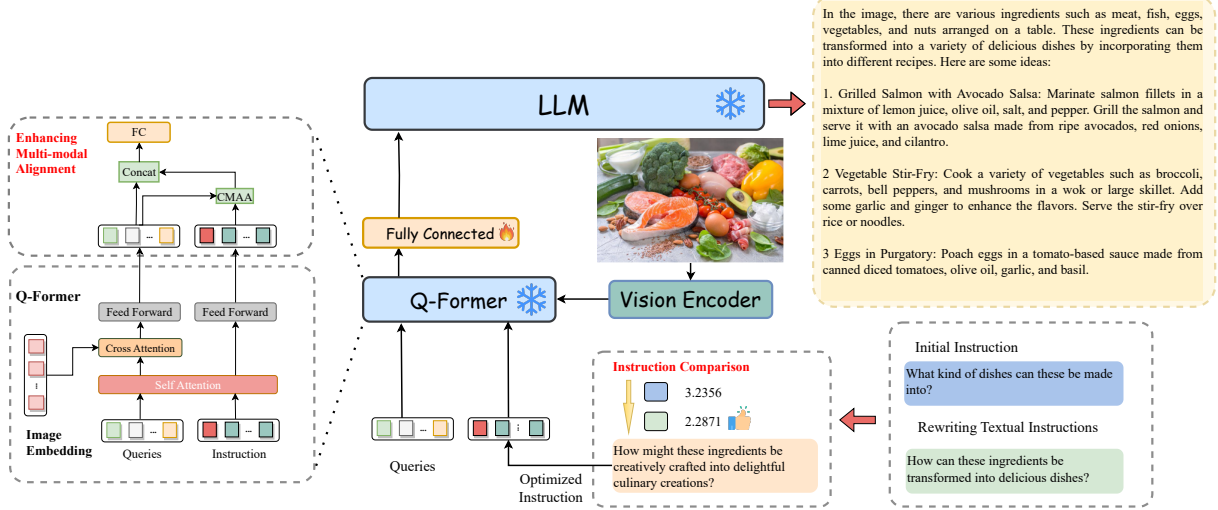


Figure 2: The figure depicts the complete workflow of Instruction Comparison Optimization. Initial and rewritten instructions are processed through comparison optimization to generate optimized instructions. Subsequently, the optimized instructions are utilized for generation in MMLMs.

tonomous Instruction Optimization (AIO).

3.1 Enhancing Multi-modal Alignment

In the quest to refine MMLMs, our focus shifts to bridging the gap between the realms of visual perception and linguistic expression. This section delves into our pioneering approach to enhancing the alignment between visual and textual modules within MMLMs, introducing a series of architectural innovations and training optimizations designed to synergize these two distinct modalities seamlessly.

Integrative Processing of Text and Image: At the core of our architectural enhancements is the integrative processing of textual and visual data. This process involves constructing a unified representation by merging detailed textual embeddings with rich visual information. We introduce the Cross-Modal Alignment Attention (CMAA) algorithm to achieve this integration, specifically designed to harmonize these disparate data modalities. This algorithm leverages attention mechanisms and cross-modal feature fusion, to ensure that the resulting multi-modal representation encapsulates both the intricacies of language and the finer details of visual content:

$$U_{mm} = \sum_{i=1}^N \text{softmax}(\text{emb}_{\text{que}} \cdot \text{emb}_{\text{text}}^T) \cdot \text{emb}_{\text{text}}(i) \quad (1)$$

where $\text{emb}_{\text{text}}(i)$ and $\text{emb}_{\text{vis}}(i)$ represent the embedding of the textual instruction and Queries

for the i -th element respectively. Simultaneously, $\text{emb}_{\text{text}}(i)$ serves as both the key (K) and value (V) in traditional attention mechanism, while $\text{emb}_{\text{vis}}(i)$ functions as the query (Q). The textual instruction, after undergoing CMAA, transforms into U_{mm} . Subsequently, U_{mm} concatenate onto the output of Queries in the form of Figure 1, culminating in the final integration of visual and textual elements.

Optimized Model Training and Performance: In developing this new architecture, our approach extends beyond mere technical integration to encompass strategic training and performance optimization. We employ selective weight freezing methods, where specific layers of the pre-trained model are kept static to preserve learned features, and targeted fine-tuning, where newly introduced components or layers are specifically trained to adapt to the task at hand. This targeted approach allows us to fine-tune the model's performance without the need for extensive retraining, thereby enhancing the learning efficiency and ensuring the robustness and scalability of the model. The loss function used for training takes the following form:

$$p(Y_{\text{text}}|X_{\text{img}}) = \prod_{i=1}^L p_{\theta}(y_i|X_{\text{img}}, Y_{\text{text}}^{[1:i-1]}) \quad (2)$$

where θ is the trainable parameters, X_{img} and Y_{text} respectively denote the input image and the output text, $Y_{\text{text}}^{[1:i-1]}$ represents the input instruction and the text already generated up to the $i - 1$ step.

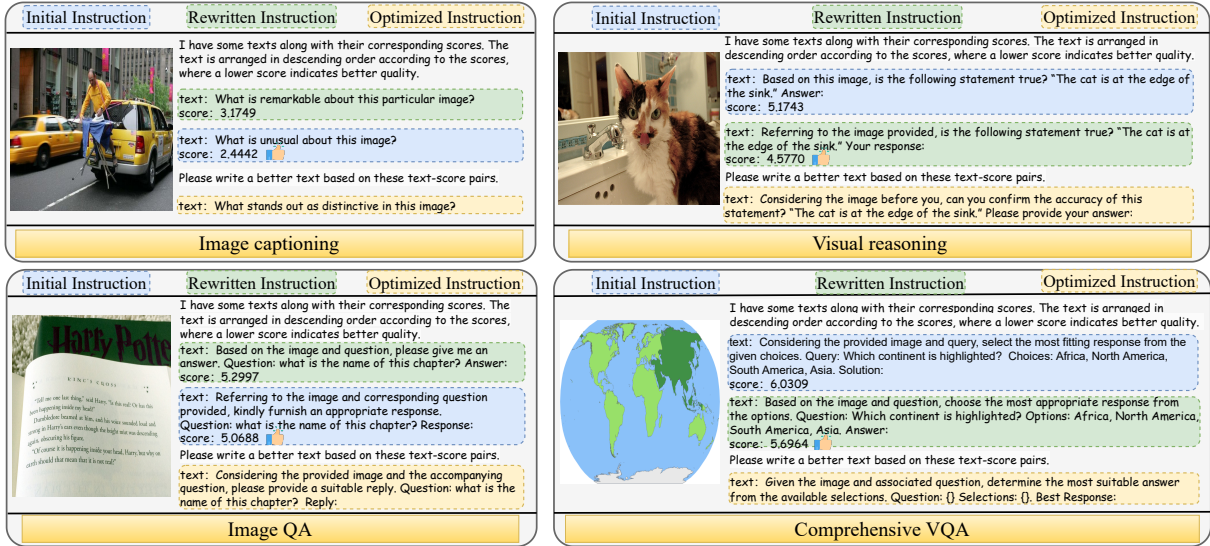


Figure 3: The examples of IAS ranking in different domains. On the left side is the image input provided to the MMLMs. On the right side, within the blue box, lies the initial instruction, while the rewritten instruction is contained within the green box. The 'score' indicates the quality of corresponding instructions with respect to the model, while the lower score (i.e., high quality) instruction always ranks later in the ICL demonstration. By utilizing the paradigm of ICL, MMLMs learn the relationship between the scores of the two cases to generate higher-quality new instructions that lie in the yellow box.

3.2 Autonomous Instruction Optimization

During inference, the textual instruction has a significant impact on the generation results of MMLMs. Therefore, we propose an approach that leverages the inherent text processing capabilities of LLMs to optimize textual instructions, thereby aligning the results generated by MMLMs more closely with user requirements. This method comprises two stages: Rewriting Textual Instructions and Instruction Alignment Optimization.

Rewriting Textual Instructions: Rewriting is the first stage in our methodology. LLMs exhibit strong text rewriting capabilities, maintaining semantic information and changing the content of the text. Therefore, our goal is to use the ability of LLM to rewrite the initial textual instructions, aiming to obtain a pair of instruction with roughly similar semantics to lay the foundation for the second stage. Furthermore, the rewritten instruction resulting from this process is not necessarily required to be of higher quality than the initial instruction. As long as there is a difference between the two, it is enough to meet the requirements of subsequent processes. This reduces the complexity of the rewrite task, making the barrier to implementation relatively low.

Specifically, we have intricately designed a prompt tailored for LLMs to rewrite textual instruction. The prompt should explicitly instruct

LLMs on how to rewrite the textual instruction while ensuring minimal semantic changes between the initial and rewritten version. The template of the prompt used in this stage can be referred to in the Appendix B. An important consideration to note is that since this stage solely involves rewriting instructions, the entire MMLMs aren't required. Involving only LLMs could slightly reduce the time consumption caused by the rewriting process.

Instruction Comparison Optimization: At this stage, we design a method that enables MMLMs to identify which instruction is better through comparative analysis and strive to generate instruction with better quality. As illustrated in Figure 2, we innovatively rank the cases in ICL so that the model can learn the quality of instructions only through the comparison between initial instruction and rewritten instruction (Ren and Liu, 2023).

Given that the ultimate goal of the instruction is to facilitate inference by MMLMs, we believe that the quality of these instructions should be evaluated by the MMLMs themselves. Specifically, we allow MMLMs to score the instruction solely by the itself without the help of external discriminator. Therefore, we proposed the Instruction Alignment Score (IAS), which is formulated to quantify the divergence between the model's predicted output and the expected output for a given instruction. We score the instruction by using a prompt

to guide MMLMs. Please see the Appendix C for the prompt template. Defined as the expectation of negative log-likelihood, IAS is calculated as follows:

$$\text{IAS} = \mathbb{E}[-\log P(t_i | X_{img}, X_{prompt}, t_{[1:i-1]}; \theta)] \quad (3)$$

Here, X_{img} is the input image, X_{prompt} denotes textual prompt employed to guide the model in its computational processes, θ represents our MMLMs model and t_i represents the textual tokens that need to be generated, which is the instruction whose quality MMLMs is tasked to evaluate. A lower IAS indicates a higher alignment of the instruction with the model’s understanding, enabling MMLMs to perform better. After calculating IAS, as shown in Figure 3, we rank the instruction-IAS pairs in descending order, and combine them into a prompt in the form of ICL to input to MMLMs to generate a optimized instruction. The optimized instruction will have better inference performance compared to the initial and rewritten instructions.

4 Experiments

4.1 Datasets

The datasets in this paper primarily consists of a training dataset and the zero-shot evaluation benchmarks. The training data is sourced from LLaVA, which is also a subset of the InstructBLIP training datasets. The data was collected by the authors of LLaVA using ChatGPT/GPT-4 (OpenAI, 2023a,b), following a multi-modal instruction format. We believe that using the same dataset as previous work enables a fairer comparison in the experiments. For an image X_v , there is an associated question-answer pair $\langle X_q, X_a \rangle$ related to X_v . In some cases, there are multi-turn dialogues represented as $(\langle X_q^1, X_a^1 \rangle, \dots, \langle X_q^m, X_a^m \rangle)$. During training, for single-turn dialogue data, X_q serves as the initial instruction, while X_a corresponds to the ground truth. Likewise, for multi-turn dialogue data, it is essential to concatenate the historical dialogues (excluding the last turn) and append them along with X_q^m as the initial instruction. Meanwhile, X_a^m serves as the ground truth.

For zero-shot evaluation benchmarks, to ensure alignment for comparison, we also follow InstructBLIP. The evaluation domains include: Image captioning: Flickr30K (Young et al., 2014), No-caps (Agrawal et al., 2019). Visual Reasoning:

VSR (Liu et al., 2023a), GQA (Hudson and Manning, 2019), IconQA (Lu et al., 2021). Image QA: VizWiz (Gurari et al., 2018), TextVQA (Mishra et al., 2019). Comprehensive VQA: Visual Dialog (Das et al., 2017), ScienceQA (Lu et al., 2022), HatefulMememes (Kiela et al., 2020). It’s important to note that for ScienceQA, we only evaluate the set with image context. The utilization of the overall evaluation benchmarks can be referenced in Appendix D. The evaluation metrics vary across benchmarks: NoCaps and Flickr30K employ CIDEr scores (Vedantam et al., 2015), HatefulMememes utilizes AUC scores, and Visual Dialog employs Mean Reciprocal Rank (MRR). For all remaining datasets, top-1 accuracy is used as the metric. All evaluation benchmarks have no data overlap with the training set, ensuring the authenticity of zero-shot. In the Appendix F, we provide the initial instructions used for all benchmarks in zero-shot learning.

4.2 Implementation details

In terms of the model architecture, we opted for the ViT-G/14 from EVA-CLIP (Fang et al., 2023) as the visual encoder, removing the final layer of the ViT and utilizing the output features from the penultimate layer. In line with InstructBLIP, we employed two distinct LLMs: FlanT5 and Vicuna. FlanT5, derived from the instruction-tuning of the encoder-decoder Transformer T5 (Raffel et al., 2020), encompasses two sizes: FlanT5-XL and FlanT5-XXL. Vicuna, on the other hand, is refined from the instruction-tuning of the decoder-only Transformer LLaMA (Touvron et al., 2023), and also includes two sizes: Vicuna-7B and Vicuna-13B. The weights of both Q-Former and the fully connected layers are sourced from InstructBLIP and need to correspond to different LLMs. Our entire model framework requires freezing the weights of the visual encoder, Q-Former, and LLMs, allowing only the fully connected layers to be unfrozen. Further details regarding training hyperparameters can be found in Appendix E.

4.3 Zero-shot Evaluation

During the evaluation process, we employed two different generation methods tailored to different benchmarks. For the domain of benchmarks such as Image Captioning, results were directly generated from instructions. These results were then compared against ground truth to calculate metrics. On the other hand, for classification-based VQA

| | Image Captioning | | Visual Reasoning | | | Image QA | | Comprehensive VQA | | |
|---------------------------------------|------------------|--------------|------------------|-------------|-------------|-------------|-------------|-------------------|-------------|-------------|
| | Flickr30K | Nocaps | VSR | GQA | IconQA | VizWiz | TextVQA | Visdial | SciQA | HM |
| BLIP-2 (FlanT5 _{XXL}) | 73.7 | 104.5 | 68.2 | 44.6 | 45.4 | 29.4 | 44.1 | 46.9 | 64.5 | 52.0 |
| BLIP-2 (Vicuna _{13B}) | 74.9 | 107.5 | 50.9 | 41.0 | 40.6 | 19.6 | 42.5 | 45.1 | 61.0 | 53.7 |
| MiniGPT-4 (Vicuna _{13B}) | / | / | 50.7 | 30.8 | 37.6 | 34.8 | 18.7 | / | / | 29.0 |
| LLaVA (Vicuna _{13B}) | / | / | 56.3 | 41.3 | 43.0 | 37.7 | 28.3 | / | / | 9.2 |
| InstructBLIP (FlanT5 _{XL}) | 84.5 | 119.9 | 64.8 | 48.4 | 50.0 | 32.7 | 46.6 | 46.6 | 70.4 | 56.6 |
| InstructBLIP (FlanT5 _{XXL}) | 83.5 | 120.0 | 65.6 | 47.9 | 51.2 | 30.9 | 46.6 | 48.5 | 70.6 | 54.1 |
| InstructBLIP (Vicuna _{7B}) | 82.4 | 123.1 | 54.3 | 49.2 | 43.1 | 34.5 | 50.1 | 45.2 | 60.5 | 59.6 |
| InstructBLIP (Vicuna _{13B}) | 82.8 | 121.9 | 52.1 | 49.5 | 44.8 | 33.4 | 50.7 | 45.4 | 63.1 | 57.5 |
| BLIVA (Vicuna _{13B}) | 87.1 | / | 62.2 | / | 44.9 | 42.9 | 58.0 | 45.6 | / | 55.6 |
| BLIVA (FlanT5 _{XXL}) | 87.7 | / | 68.8 | / | 52.4 | 44.0 | 57.2 | 36.2 | / | 50.0 |
| Ours(FlanT5 _{XL}) | 85.3 | 119.5 | 64.1 | 47.9 | 50.4 | 33.0 | 48.7 | 47.0 | 71.0 | 60.0 |
| Ours(FlanT5 _{XXL}) | 88.5 | 120.4 | 66.9 | 48.1 | 51.2 | 31.3 | 48.8 | 49.2 | 81.8 | 55.7 |
| Ours(Vicuna _{7B}) | 87.9 | 124.2 | 60.1 | 52.0 | 44.2 | 42.7 | 60.6 | 45.7 | 74.6 | 62.7 |
| Ours(Vicuna _{13B}) | 84.0 | 119.8 | 56.2 | 52.9 | 50.3 | 45.0 | 65.6 | 45.7 | 71.0 | 58.9 |

Table 1: Zero-shot results on general VQA benchmarks. Here, Visdial, SciQA, and HM respectively refer to Visual Dialog, ScienceQA, and HatefulMemes. The results for MiniGPT-4 and LLaVA are sourced from BLIVA (Hu et al., 2023), while the remaining results originate from their respective papers (Li et al., 2023; Dai et al., 2023).

tasks, we followed previous work (Alayrac et al., 2022; Dai et al., 2023) by computing the language model loss for each candidate option and selecting the one with the lowest loss as the final prediction. This method was applied to ScienceQA, IconQA, HatefulMemes, and Visual Dialog.

We conducted zero-shot learning of our model against previous state-of-the-art works across 10 benchmarks in Table 1. It’s evident that our model showcases a significant advantage across the majority of benchmarks, especially in Image QA and Comprehensive VQA domains. At the same time, due to the primary inheritance of our model weights from InstructBLIP, a horizontal comparison with InstructBLIP reveals that our method significantly strengthens the generative capability of MMLMs. For instance, with model based on FlanT5-XXL, our approach exhibits a comparative increase of 6.0% and 15.9% in performance over InstructBLIP concerning Flickr30K and ScienceQA, respectively. These results demonstrate that the instruction optimization approach we proposed exhibits highly favorable gains for multi-modal tasks in the domain of image-text.

4.4 Ablation study

To investigate the impact of Enhancing Multi-modal Alignment (EMA, Section 3.1) and Autonomous Instruction Optimization (AIO, Section 3.2) on the final results, we conducted ablation studies by individually removing them during eval-

uation.

As depicted in Table 2, after integrating the EMA mechanism on the vanilla baseline, the overall performance of all models is significantly enhanced. This indicates that our EMA method indeed enhances the alignment between images and text. Moreover, if AIO continues to be integrated on the basis of EMA, the evaluation results can be further improved. This adequately shows that the two mechanisms can strengthen each other. EMA, by enhancing its perception of instructions, can serve as a booster to further enhance AIO.

As for the AIO part, we also further split it to conduct ablation experiments. We discuss Rewriting Textual Instructions and Instruction Comparison Optimization separately. It can be clearly seen from the results in Table 2 that instruction rewriting cannot continue to improve the effect on the basis of EMA. On the contrary, it is even inferior to the vanilla baseline in many results. This phenomenon fully demonstrates that just rewriting cannot stably optimize the instruction, and requires correction by our Instruction Comparison Optimization mechanism.

4.5 Qualitative evaluation

Beyond the benchmarks-driven experimental analyses, we diversified our qualitative evaluation by incorporating real-world images and instructions. As shown in Figure 4, we have enumerated three cases for comprehensive analysis. The process



Figure 4: The one on the left is a case written for a product advertisement, the one in the middle is a recipe description, and the one on the right is a poetry creation. Qualitative comparison of three responses from different ablations: initial instruction with vanilla model (blue), initial instruction with EMA model (purple), and optimized instruction with EMA model (green).

| Vanilla | EMA | AIO | | Image Captioning | | Visual Reasoning | | | Image QA | | Comprehensive VQA | | |
|-------------------|-----|-----------|------------|------------------|--------------|------------------|-------------|-------------|-------------|-------------|-------------------|-------------|-------------|
| | | Rewriting | Comparison | Flickr30K | Nocaps | VSR | GQA | IconQA | VizWiz | TextVQA | Visdial | SciQA | HM |
| <i>FlaxT5-XL</i> | | | | | | | | | | | | | |
| ✓ | | | | 84.5 | 119.9 | 64.8 | 48.4 | 50.0 | 32.7 | 46.6 | 46.6 | 70.4 | 56.6 |
| ✓ | ✓ | | | 85.1 | 119.7 | 63.5 | 48.6 | 50.0 | 32.8 | 48.5 | 46.9 | 70.6 | 60.8 |
| ✓ | ✓ | ✓ | | 84.7 | 118.1 | 66.8 | 48.5 | 49.0 | 31.8 | 47.5 | 44.8 | 70.4 | 57.3 |
| ✓ | ✓ | ✓ | ✓ | 85.3 | 119.5 | 64.1 | 47.9 | 50.4 | 33.0 | 48.7 | 47.0 | 71.0 | 60.0 |
| <i>FlaxT5-XXL</i> | | | | | | | | | | | | | |
| ✓ | | | | 83.5 | 120.0 | 65.6 | 47.9 | 51.2 | 30.9 | 46.6 | 48.5 | 70.6 | 54.1 |
| ✓ | ✓ | | | 86.3 | 120.3 | 55.7 | 48.0 | 51.6 | 31.5 | 48.3 | 49.0 | 82.0 | 55.2 |
| ✓ | ✓ | ✓ | | 85.3 | 120.1 | 66.5 | 48.1 | 50.9 | 31.1 | 46.7 | 48.5 | 73.5 | 54.1 |
| ✓ | ✓ | ✓ | ✓ | 88.5 | 120.4 | 66.9 | 48.3 | 51.2 | 31.3 | 48.8 | 49.2 | 81.8 | 55.7 |
| <i>Vicuna-7B</i> | | | | | | | | | | | | | |
| ✓ | | | | 82.4 | 123.1 | 54.3 | 49.2 | 43.1 | 34.5 | 50.1 | 45.2 | 60.5 | 59.6 |
| ✓ | ✓ | | | 81.6 | 124.5 | 60.6 | 51.9 | 43.2 | 40.5 | 49.9 | 45.3 | 55.4 | 60.8 |
| ✓ | ✓ | ✓ | | 82.3 | 124.5 | 55.4 | 47.6 | 44.0 | 40.3 | 58.3 | 43.4 | 63.0 | 62.2 |
| ✓ | ✓ | ✓ | ✓ | 87.9 | 124.2 | 60.1 | 52.0 | 44.2 | 42.7 | 60.6 | 45.7 | 74.6 | 62.7 |
| <i>Vicuna-13B</i> | | | | | | | | | | | | | |
| ✓ | | | | 82.8 | 121.9 | 52.1 | 49.5 | 44.8 | 33.4 | 50.7 | 45.4 | 63.1 | 57.5 |
| ✓ | ✓ | | | 84.4 | 120.2 | 58.9 | 51.6 | 48.4 | 43.0 | 56.9 | 43.0 | 48.4 | 61.0 |
| ✓ | ✓ | ✓ | | 80.4 | 120.6 | 52.5 | 51.1 | 49.3 | 41.5 | 62.4 | 44.4 | 68.0 | 58.7 |
| ✓ | ✓ | ✓ | ✓ | 84.0 | 120.8 | 56.2 | 52.9 | 50.3 | 45.0 | 65.6 | 45.7 | 71.0 | 58.9 |

Table 2: Results of ablation studies for Enhancing Multi-modal Alignment (EMA) and Autonomous Instruction Optimization (AIO) in different LLMs models. Among them, EMA is split into Rewriting Textual Instructions (Rewriting) and Instruction Comparison Optimization (Comparison) for discussion respectively. Vanilla represents the baseline model without any of our proposed modules and ✓ indicates that the module has been integrated.

424 commences with the input of an image, subsequent
425 questions and answers revolve around this visual
426 context. This is followed by the presentation of
427 instructions, encompassing both the initial instruc-
428 tions and the optimized by the AIO module. Con-
429 clusively, model response is delineated. The output
430 section for evaluation includes: the results obtained
431 by inputting the initial instructions into the vanilla
432 model (Vanilla Response); the results obtained by
433 inputting the initial instructions into the integrated
434 EMA module model (EMA Response); and the re-
435 sults from inputting the optimized instructions into
436 the integrated EMA module model (EMA & AIO
437 Response), which is VisLingInstruct.

438 The outcome as observed in the figure suggests
439 that the EMA Response demonstrates an improve-
440 ment over the Vanilla Response, both in terms of
441 content accuracy and richness of detail. For in-
442 stance, within the case of poetry creation, the erro-
443 neously presented ‘3 huts’ is accurately identified
444 as ‘a small house’. In the case of recipe descrip-
445 tion, the narrative about spaghetti is much more
446 detailed in the EMA Response. Furthermore, the
447 EMA & AIO response also surpasses the EMA re-
448 sponse alone, evident in the former’s answers pos-
449 sessing

449 a superior logical organization and better fulfill-
450 ment of user intent. This is well illustrated in all
451 three cases presented in the figure. And for more
452 on the performance in multi-turn dialogues, we
453 have provided a demonstration and discussion in
454 the Appendix G.

455 5 Conclusion

456 This paper proposes VisLingInstruct, a novel au-
457 tonomous instruction optimization framework for
458 visual-linguistic multi-modal models. We con-
459 ducted a comprehensive study on multi-modal mod-
460 els and demonstrated the powerful autonomous in-
461 struction optimization capabilities of the VisLingIn-
462 struct model, demonstrating strong zero-shot learn-
463 ing capabilities in a series of benchmarks. At the
464 end of the experiment, qualitative examples were
465 used to demonstrate the specific situation of VisLing-
466 Instruct in autonomous instruction optimization,
467 such as knowledge-based image description, image-
468 based text creation and multi-turn dialogue. We
469 hope that VisLingInstruct can inspire more new re-
470 search on autonomous optimization of multi-modal
471 instruction.

472 Limitations

473 Limitations of the current work are discussed below.
474 Firstly, while the proposed multimodal autonomous
475 instruction optimization framework performs well
476 in terms of effectiveness, its structure is relatively
477 intricate. Streamlining the process while maintain-
478 ing effectiveness would greatly facilitate the prac-
479 tical application of this technology. Secondly, the
480 experiments in this paper are focused on image and
481 text modalities, and further validation is needed to
482 determine the effectiveness of our framework in
483 other modalities, such as video and audio.

484 References

485 Harsh Agrawal, Karan Desai, Yufei Wang, Xinlei Chen,
486 Rishabh Jain, Mark Johnson, Dhruv Batra, Devi
487 Parikh, Stefan Lee, and Peter Anderson. 2019. No-
488 caps: Novel object captioning at scale. In *Proceed-*
489 *ings of the IEEE/CVF international conference on*
490 *computer vision*, pages 8948–8957.

491 Jean-Baptiste Alayrac, Jeff Donahue, Pauline Luc,
492 Antoine Miech, Iain Barr, Yana Hasson, Karel
493 Lenc, Arthur Mensch, Katherine Millican, Malcolm
494 Reynolds, et al. 2022. Flamingo: a visual language
495 model for few-shot learning. *Advances in Neural*
496 *Information Processing Systems*, 35:23716–23736.

497 Tom Brown, Benjamin Mann, Nick Ryder, Melanie
498 Subbiah, Jared D Kaplan, Prafulla Dhariwal, Arvind
499 Neelakantan, Pranav Shyam, Girish Sastry, Amanda
500 Askell, et al. 2020. Language models are few-shot
501 learners. *Advances in neural information processing*
502 *systems*, 33:1877–1901.

503 Xi Chen, Xiao Wang, Soravit Changpinyo, AJ Pier-
504 giovanni, Piotr Padlewski, Daniel Salz, Sebastian
505 Goodman, Adam Grycner, Basil Mustafa, Lucas
506 Beyer, et al. 2022. Pali: A jointly-scaled mul-
507 tilingual language-image model. *arXiv preprint*
508 *arXiv:2209.06794*.

509 Daixuan Cheng, Shaohan Huang, Junyu Bi, Yuefeng
510 Zhan, Jianfeng Liu, Yujing Wang, Hao Sun, Furu Wei,
511 Denvy Deng, and Qi Zhang. 2023. Uprise: Universal
512 prompt retrieval for improving zero-shot evaluation.
513 *arXiv preprint arXiv:2303.08518*.

514 Hyung Won Chung, Le Hou, Shayne Longpre, Barret
515 Zoph, Yi Tay, William Fedus, Yunxuan Li, Xuezhi
516 Wang, Mostafa Dehghani, Siddhartha Brahma, et al.
517 2022. Scaling instruction-finetuned language models.
518 *arXiv preprint arXiv:2210.11416*.

519 Wenliang Dai, Junnan Li, Dongxu Li, Anthony
520 Meng Huat Tiong, Junqi Zhao, Weisheng Wang,
521 Boyang Li, Pascale Fung, and Steven Hoi. 2023. In-
522 structblip: Towards general-purpose vision-language
523 models with instruction tuning. *arXiv preprint*
524 *arXiv:2305.06500*.

Abhishek Das, Satwik Kottur, Khushi Gupta, Avi Singh,
Deshraj Yadav, José MF Moura, Devi Parikh, and
Dhruv Batra. 2017. Visual dialog. In *Proceedings of*
the IEEE conference on computer vision and pattern
recognition, pages 326–335. 525
526
527
528
529

Yuxin Fang, Wen Wang, Binhui Xie, Quan Sun, Ledell
Wu, Xinggang Wang, Tiejun Huang, Xinlong Wang,
and Yue Cao. 2023. Eva: Exploring the limits of
masked visual representation learning at scale. In
Proceedings of the IEEE/CVF Conference on Com-
puter Vision and Pattern Recognition, pages 19358–
19369. 530
531
532
533
534
535
536

Tianyu Gao, Adam Fisch, and Danqi Chen. 2021.
Making pre-trained language models better few-shot
learners. In *Joint Conference of the 59th Annual*
Meeting of the Association for Computational Lin-
guistics and the 11th International Joint Conference
on Natural Language Processing, ACL-IJCNLP 2021,
pages 3816–3830. 537
538
539
540
541
542
543

Danna Gurari, Qing Li, Abigale J Stangl, Anhong Guo,
Chi Lin, Kristen Grauman, Jiebo Luo, and Jeffrey P
Bigham. 2018. Vizwiz grand challenge: Answering
visual questions from blind people. In *Proceedings of*
the IEEE conference on computer vision and pattern
recognition, pages 3608–3617. 544
545
546
547
548
549

Wenbo Hu, Yifan Xu, Y Li, W Li, Z Chen, and Z Tu.
2023. Bliva: A simple multimodal llm for better
handling of text-rich visual questions. *arXiv preprint*
arXiv:2308.09936. 550
551
552
553

Drew A Hudson and Christopher D Manning. 2019.
Gqa: A new dataset for real-world visual reasoning
and compositional question answering. In *Proceed-*
ings of the IEEE/CVF conference on computer vision
and pattern recognition, pages 6700–6709. 554
555
556
557
558

Jacob Devlin Ming-Wei Chang Kenton and Lee Kristina
Toutanova. 2019. Bert: Pre-training of deep bidirec-
tional transformers for language understanding. In
Proceedings of NAACL-HLT, pages 4171–4186. 559
560
561
562

Douwe Kiela, Hamed Firooz, Aravind Mohan, Vedanuj
Goswami, Amanpreet Singh, Pratik Ringshia, and
Davide Testuggine. 2020. The hateful memes chal-
lenge: Detecting hate speech in multimodal memes.
Advances in neural information processing systems,
33:2611–2624. 563
564
565
566
567
568

Dongxu Li, Junnan Li, Hung Le, Guangsen Wang, Sil-
vio Savarese, and Steven CH Hoi. 2022. Lavis: A li-
brary for language-vision intelligence. *arXiv preprint*
arXiv:2209.09019. 569
570
571
572

Junnan Li, Dongxu Li, Silvio Savarese, and Steven Hoi.
2023. Blip-2: Bootstrapping language-image pre-
training with frozen image encoders and large lan-
guage models. *arXiv preprint arXiv:2301.12597*. 573
574
575
576

Fangyu Liu, Guy Emerson, and Nigel Collier. 2023a.
Visual spatial reasoning. *Transactions of the Associ-*
ation for Computational Linguistics, 11:635–651. 577
578
579

| | | | |
|-----|---|--|-----|
| 580 | Haotian Liu, Chunyuan Li, Qingyang Wu, and Yong Jae Lee. 2023b. Visual instruction tuning. <i>arXiv preprint arXiv:2304.08485</i> . | Faisal Azhar, et al. 2023. Llama: Open and efficient foundation language models. <i>arXiv preprint arXiv:2302.13971</i> . | 634 |
| 581 | | | 635 |
| 582 | | | 636 |
| 583 | Ilya Loshchilov and Frank Hutter. 2018. Decoupled weight decay regularization. In <i>International Conference on Learning Representations</i> . | Ramakrishna Vedantam, C Lawrence Zitnick, and Devi Parikh. 2015. Cider: Consensus-based image description evaluation. In <i>Proceedings of the IEEE conference on computer vision and pattern recognition</i> , pages 4566–4575. | 637 |
| 584 | | | 638 |
| 585 | | | 639 |
| 586 | Jinghui Lu, Dongsheng Zhu, Weidong Han, Rui Zhao, Brian Mac Namee, and Fei Tan. 2023. What makes pre-trained language models better zero-shot learners? In <i>Proceedings of the 61st Annual Meeting of the Association for Computational Linguistics</i> , pages 2288–2303. | Jason Wei, Xuezhi Wang, Dale Schuurmans, Maarten Bosma, Fei Xia, Ed Chi, Quoc V Le, Denny Zhou, et al. 2022. Chain-of-thought prompting elicits reasoning in large language models. <i>Advances in Neural Information Processing Systems</i> , 35:24824–24837. | 642 |
| 587 | | | 643 |
| 588 | | | 644 |
| 589 | | | 645 |
| 590 | | | 646 |
| 591 | | | |
| 592 | Pan Lu, Swaroop Mishra, Tanglin Xia, Liang Qiu, Kai-Wei Chang, Song-Chun Zhu, Oyvind Tafjord, Peter Clark, and Ashwin Kalyan. 2022. Learn to explain: Multimodal reasoning via thought chains for science question answering. <i>Advances in Neural Information Processing Systems</i> , 35:2507–2521. | Chengrun Yang, Xuezhi Wang, Yifeng Lu, Hanxiao Liu, Quoc V Le, Denny Zhou, and Xinyun Chen. 2023. Large language models as optimizers. <i>arXiv preprint arXiv:2309.03409</i> . | 647 |
| 593 | | | 648 |
| 594 | | | 649 |
| 595 | | | 650 |
| 596 | | | 651 |
| 597 | | | 652 |
| 598 | Pan Lu, Liang Qiu, Jiaqi Chen, Tony Xia, Yizhou Zhao, Wei Zhang, Zhou Yu, Xiaodan Liang, and Song-Chun Zhu. 2021. Iconqa: A new benchmark for abstract diagram understanding and visual language reasoning. <i>arXiv preprint arXiv:2110.13214</i> . | Qinghao Ye, Haiyang Xu, Guohai Xu, Jiabo Ye, Ming Yan, Yiyang Zhou, Junyang Wang, Anwen Hu, Pengcheng Shi, Yaya Shi, et al. 2023. mplug-owl: Modularization empowers large language models with multimodality. <i>arXiv preprint arXiv:2304.14178</i> . | 653 |
| 599 | | | 654 |
| 600 | | | 655 |
| 601 | | | 656 |
| 602 | | | |
| 603 | Sewon Min, Xinxu Lyu, Ari Holtzman, Mikel Artetxe, Mike Lewis, Hannaneh Hajishirzi, and Luke Zettlemoyer. 2022. Rethinking the role of demonstrations: What makes in-context learning work? In <i>Proceedings of the 2022 Conference on Empirical Methods in Natural Language Processing</i> , pages 11048–11064. | Peter Young, Alice Lai, Micah Hodosh, and Julia Hockenmaier. 2014. From image descriptions to visual denotations: New similarity metrics for semantic inference over event descriptions. <i>Transactions of the Association for Computational Linguistics</i> , 2:67–78. | 657 |
| 604 | | | 658 |
| 605 | | | 659 |
| 606 | | | 660 |
| 607 | | | 661 |
| 608 | | | |
| 609 | Anand Mishra, Shashank Shekhar, Ajeet Kumar Singh, and Anirban Chakraborty. 2019. Ocr-vqa: Visual question answering by reading text in images. In <i>2019 international conference on document analysis and recognition (ICDAR)</i> , pages 947–952. | Huaixiu Steven Zheng, Swaroop Mishra, Xinyun Chen, Heng-Tze Cheng, Ed H Chi, Quoc V Le, and Denny Zhou. 2023a. Take a step back: Evoking reasoning via abstraction in large language models. <i>arXiv preprint arXiv:2310.06117</i> . | 662 |
| 610 | | | 663 |
| 611 | | | 664 |
| 612 | | | 665 |
| 613 | | | 666 |
| 614 | OpenAI. 2023a. Chatgpt . Technical report. | Lianmin Zheng, Wei-Lin Chiang, Ying Sheng, Siyuan Zhuang, Zhanghao Wu, Yonghao Zhuang, Zi Lin, Zhuohan Li, Dacheng Li, Eric P Xing, Hao Zhang, Joseph E. Gonzalez, and Ion Stoica. 2023b. Judging llm-as-a-judge with mt-bench and chatbot arena. <i>arXiv preprint arXiv:2306.05685</i> . | 667 |
| 615 | OpenAI. 2023b. Gpt-4 . Technical report. | | 668 |
| 616 | Long Ouyang, Jeffrey Wu, Xu Jiang, Diogo Almeida, Carroll Wainwright, Pamela Mishkin, Chong Zhang, Sandhini Agarwal, Katarina Slama, Alex Ray, et al. 2022. Training language models to follow instructions with human feedback. <i>Advances in Neural Information Processing Systems</i> , 35:27730–27744. | | 669 |
| 617 | | | 670 |
| 618 | | | 671 |
| 619 | | | 672 |
| 620 | | | |
| 621 | | | |
| 622 | Colin Raffel, Noam Shazeer, Adam Roberts, Katherine Lee, Sharan Narang, Michael Matena, Yanqi Zhou, Wei Li, and Peter J Liu. 2020. Exploring the limits of transfer learning with a unified text-to-text transformer. <i>The Journal of Machine Learning Research</i> , 21(1):5485–5551. | Deyao Zhu, Jun Chen, Xiaoqian Shen, Xiang Li, and Mohamed Elhoseiny. 2023. Minigpt-4: Enhancing vision-language understanding with advanced large language models. <i>arXiv preprint arXiv:2304.10592</i> . | 673 |
| 623 | | | 674 |
| 624 | | | 675 |
| 625 | | | 676 |
| 626 | | | |
| 627 | | | |
| 628 | Ruifeng Ren and Yong Liu. 2023. In-context learning with transformer is really equivalent to a contrastive learning pattern. <i>arXiv preprint arXiv:2310.13220</i> . | | |
| 629 | | | |
| 630 | | | |
| 631 | Hugo Touvron, Thibaut Lavril, Gautier Izacard, Xavier Martinet, Marie-Anne Lachaux, Timothée Lacroix, Baptiste Rozière, Naman Goyal, Eric Hambro, | | |
| 632 | | | |
| 633 | | | |

A Algorithm

A.1 Algorithm Overview

The algorithmic core of our approach in VisLingInstruct is structured around two main processes: Cross-Modal Alignment Attention and Autonomous Instruction Optimization. The former process harmonizes the integration of text and image, while the latter refines the textual instructions for MMLMs.

A.2 Cross-Modal Alignment Attention

The Cross-Modal Alignment Attention (CMAA) algorithm focuses on the integration of textual and visual embeddings, creating a unified text representation.

Algorithm 1 Cross-Modal Alignment Attention

Require: Textual embeddings E_{text} , Queries embeddings E_{que}
Ensure: Unified multi-modal representation U_{mm}
1: Initialize cross-modal alignment mechanism
2: **for** each element i in E_{text} **do**
3: Compute attention between $E_{\text{text}}(i)$ and E_{que}
4: Assign attention weight on $E_{\text{text}}(i)$
5: **end for**
6: $U_{\text{mm}} \leftarrow$ Aggregate of aligned and weighted E_{text} **return** U_{mm}

A.3 Autonomous Instruction Optimization

The Autonomous Instruction Optimization (AIO) is designed to transform initial instruction into an optimized format.

Algorithm 2 Autonomous Instruction Optimization

Require: Initial instructions I_i
Ensure: optimized instruction I_{opt}
1: Initialize autonomous instruction optimization
2: Rewriting the initial instruction I_i to obtain I_j
3: Calculating the IAS for I_i and I_j
4: Ranking the instruction-IAS pairs
5: $I_{\text{refined}} \leftarrow$ Constructing the prompt input for Instruction Comparison in MMLMs **return** I_{refined}

B Instruction rewriting templates

Here is the template used for Instruction rewriting in this paper, where ‘{ }’ signifies the instruction

that requires modification:

There is the text { }. Please modify the text to make it better while retaining the sentence structure and keywords.

C IAS templates

In the following prompt template, { } is used to place instructions requiring MPG calculation.

<Image>Based on the image given, the most appropriate instruction should be: { }

D Zero-shot evaluation datasets details

| Dataset Name | Part | count |
|----------------|----------|-------|
| Flickr30K | test | 1000 |
| NoCaps | val | 4500 |
| VSR | test | 1222 |
| GQA | test-dev | 12578 |
| IconQA | test | 6316 |
| VizWiz | test-dev | 4319 |
| TextVQA | val | 5000 |
| Visual Dialog | val | 2064 |
| ScienceQA | test | 2017 |
| HatefulMememes | val | 1040 |

Table 3: The selected part in all zero-shot evaluation benchmarks, and accompanied by specific data count.

E Training details

We implement VisLingInstruct by LAVIS library (Li et al., 2022). We fine-tuned the fully connected layers for 3 epochs, employing different hyperparameters across distinct LLMs. We employ a batch size of 32, 128 and 256 for the Vicuna-7B/13B, FlanT5-XL and FlanT5-XXL, respectively. For each model, we conduct validation every 1K steps. A consistent aspect across our training procedures was the utilization of the AdamW (Loshchilov and Hutter, 2018) optimizer with $\beta_1 = 0.9$, $\beta_2 = 0.999$, and a weight decay of 0.05. Furthermore, we implemented a linear warm-up of the learning rate over the initial 1K steps, escalating from 10^{-8} to 10^{-5} , followed by cosine decay towards a minimum learning rate of 0.

All our model’s trainable parameter counts are maintained within the range of a few million. Under the conditions of 8 A100 40G, the training durations for FlanT5, Vicuna 7B, and Vicuna 13B

| Dataset | Initial instruction |
|----------------------|--|
| Flickr30K/ NoCaps | <Image>A short image description: |
| VSR | <Image>Based on the image, is this statement true or false? {} |
| GQA/ Visdial | <Image>Question: {} \n Short answer: |
| IconQA | <Image>Question: {} Options: {} \n Answer: |
| VizWiz | <Image>Answer the question based on the image. Reply in one phrase/word or say 'unanswerable'. Question: {} \n Short answer: |
| TextVQA | <Image>OCR tokens: {} Question: \n Short answer: |
| SciQA | <Image>Given the image, choose the correct option for the following question. Question: {} \n Options: {} |
| HM | <Image>This is an image with: {} written on it. Is it hateful? |

Table 4: Presentation of initial instructions for each benchmark.

are 105 minutes, 135 minutes, and 210 minutes, respectively.

F Instructions in benchmarks

Table 4 illustrates the initial instructions for all benchmarks. The initial instructions were predominantly sourced from InstructBLIP. ‘{}’ contains entities such as questions from each individual case. For instructions with options, we separate the choices alphabetically, for instance: (a) apple (b) banana (c) pineapple.

G Multi-turn dialogues case studies

As illustrated in Figures 5 and 6, we present additional cases regarding multi-turn dialogue to showcase the strengths and distinctive features of our approach. The multi-turn generation results on the right originate from the models incorporating the EMA and AIO proposed in this paper (VisLingInstruct), while those on the left exclude this aspect, representing the results from Vanilla Response.


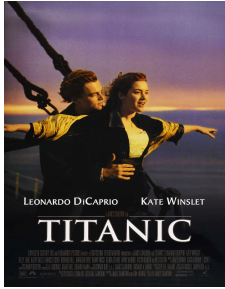

| | |
|--|---|
|  |  |
| <p>Can you give me a short introduction about the movie?</p> | <p>Would you mind offering a brief synopsis of the film?</p> |
| <p>A poster for the movie titanic.</p> | <p>Titanic is a romantic drama film directed by James Cameron and released in 1997. The movie tells the story of two young lovers, Jack Dawson (played by Leonardo DiCaprio) and Rose DeWitt Bukater (played by Kate Winslet), who fall in love aboard the ill-fated RMS Titanic during its maiden voyage in 1912. The film explores themes of love, sacrifice, and survival amidst the tragedy of the ship's sinking, which remains one of the deadliest maritime disasters in history.</p> |
| <p>Can you give me a short introduction about the movie?</p> | <p>Can you give me a short introduction about the movie?</p> |
| <p>The movie titanic was released in 1997 and became one of the highest-grossing movies of all time, grossing over \$2 billion worldwide.</p> | <p>Titanic is widely regarded as a classic romantic drama film that captivated audiences worldwide upon its release in 1997. The film's breathtaking visuals, heart-wrenching storyline, and memorable performances by its lead actors, Leonardo DiCaprio and Kate Winslet, have contributed to its enduring popularity. Many viewers were moved by the film's portrayal of young love amidst the tragedy of the Titanic's sinking, which serves as a poignant reminder of the fragility of life and the importance of cherishing every moment. Additionally, the film's attention to historical accuracy and meticulous re-creation of the Titanic's maiden voyage added depth and authenticity to an already captivating story. Overall, Titanic has left a lasting impact on audiences, becoming one of the highest-grossing films of all time and winning numerous awards, including 11 Academy Awards nominations and 11 wins, including Best Picture and Best Director for James Cameron.</p> |
| <p>Can you recommend me some other similar movies?</p> | <p>Can you recommend me some other similar movies?</p> |
| <p>1. Titanic (1997) 2. Avatar (2009) 3. The Lord of the Rings: The Fellowship of the Ring (2001) 4. Harry Potter and the Philosopher's Stone (2001) 5. Jurassic Park (1993)</p> | <p>1. The Great Gatsby (2013) - A romantic drama film directed by Baz Luhrmann and starring Leonardo DiCaprio as Jay Gatsby, a wealthy young man who falls in love with Daisy Buchanan (played by Carey Mulligan). 2. Romeo + Juliet (1996) - A romantic tragedy film directed by Baz Luhrmann and starring Leonardo DiCaprio as Romeo Montague and Claire Danes as Juliet Capulet. 3. The Notebook (2004) - A romantic drama film directed by Nick Cassavetes and starring Ryan Gosling as Noah Calhoun and Rachel McAdams as Allie Hamilton. 4. A Walk to Remember (2002) - A romantic drama film directed by Adam Shankman and starring Mandy Moore as Jamie Sullivan and Shane West as Landon Carter. 5. The Fault in Our Stars (2014) - A romantic drama that follows the story of two teenagers, played by Shailene Woodley and Ansel Elgort, who fall in love while dealing with terminal illnesses.</p> |

Figure 5: This multi-turn dialogue example demonstrates the effectiveness of VisLingInstruct in movie introduction and recommendation. Our generated results (right) exhibit significantly improved accuracy in identifying instructional content and richness in answers compared to the vanilla model's results (left).



How should I make this food?

To make this meal, you would need the following ingredients: steak, broccoli, tomatoes, and dipping sauce. First, cook the steak to your desired level of doneness. Then, chop the broccoli and tomatoes into bite-sized pieces. Finally, serve the steak with the vegetables and dipping sauce on a plate.


Is there anything I need to pay attention to?

Yes, it's important to pay attention to the cooking time and temperature of the steak to ensure that it is cooked to your desired level of doneness. Overcooking or undercooking the steak can affect its texture, taste, and overall quality. To avoid this, use a meat thermometer to check the internal temperature of the steak and adjust the cooking time accordingly.

Are there any foods that go well with this dish?

Yes, there are several foods that go well with this steak and vegetable dish. Here are a few suggestions:

1. Rice or pasta: Adding a side of rice or pasta to the meal can provide additional carbohydrates and complement the flavors of the steak and vegetables.
2. Potatoes: Roasted or mashed potatoes can be a great addition to the meal, especially if you prefer a heartier dish.
3. Salad: Adding a salad made with greens, vegetables, and a light vinaigrette dressing can provide a refreshing contrast to the rich flavors of the steak and dipping sauce.
4. Bread or rolls: Serving the steak and vegetables with a side of bread or rolls can make for a satisfying sandwich-style meal.



What's the best approach to cooking this dish?

The best approach to cooking this dish, which consists of a steak, broccoli, and tomatoes, would be to ensure that the ingredients are cooked evenly and thoroughly. This can be achieved by using a variety of cooking techniques, such as grilling, pan-frying, or oven-roasting the steak. For the broccoli and tomatoes, they can be sautéed or steamed to retain their texture and flavor. Additionally, it's important to season the dish with appropriate spices or sauces to enhance its taste and make it more appealing to the diner.

When considering key factors, what should I be particularly aware of?

When considering key factors for cooking the dish consisting of a steak, broccoli, and tomatoes, there are several aspects to keep in mind: **1. Timing:** Ensure that each ingredient is cooked at the appropriate time to avoid overcooking or undercooking any of them. The steak should be cooked to the desired level of doneness, while the broccoli and tomatoes should be cooked just enough to retain their texture and flavor. **2. Temperature:** Maintaining a consistent temperature throughout the cooking process is crucial to ensure that the ingredients are cooked evenly and thoroughly. This can be achieved by using a thermometer to monitor the temperature of the grill, pan, or oven during cooking. **3. Seasoning:** Properly seasoning the dish with appropriate spices or sauces can enhance its taste and make it more appealing to the diner. Experiment with different combinations of herbs, spices, and sauces to find the perfect blend that complements the flavors of the steak, broccoli, and tomatoes.

What are some ideal food pairings for this dish?

Some ideal food pairings for the dish consisting of a steak, broccoli, and tomatoes include:

1. Red wine: A full-bodied red wine, such as Cabernet Sauvignon or Merlot, can complement the rich flavors of the steak and enhance the overall taste of the dish.
2. Potatoes: Roasted or mashed potatoes can be a great side dish to balance the flavors and textures of the steak, broccoli, and tomatoes.
3. Green salad: Adding a simple green salad with a light vinaigrette dressing can provide a refreshing contrast to the rich flavors of the steak and vegetables.
4. Bread: A crusty bread or roll can be used to soak up the juices from the steak and vegetables, adding an extra layer of flavor and texture to the dish.

Figure 6: This is a multi-turn dialogue about cooking topics. The two generated answers exhibit similar accuracy in content recognition. However, in terms of richness and the final food pairing, our response (right) surpasses the vanilla model's response (left) significantly